SoftwareX 23 (2023) 101453

Contents lists available at ScienceDirect

SoftwareX

journal homepage: www.elsevier.com/locate/softx

Original software publication

"shortCardiac" — An open-source framework for fast and standardized assessment of cardiac function

Karl Ludger Radke [a,*], Janina Hußmann [a,b], Lena Röwer [a,b], Dirk Voit [c], Jens Frahm [c], Gerald Antoch [a], Dirk Klee [a], Frank Pillekamp [a,b], Hans-Jörg Wittsack [a]

[a] Department of Diagnostic and Interventional Radiology, Medical Faculty, University Dusseldorf, D-40225 Düsseldorf, Germany
[b] Department of General Pediatrics, Neonatology and Pediatric Cardiology, University Children's Hospital Düsseldorf, D-40225 Düsseldorf, Germany
[c] Biomedical NMR, Max Planck Institute for Multidisciplinary Sciences, D-37070 Göttingen, Germany

ARTICLE INFO

Article history:
Received 6 December 2022
Received in revised form 16 June 2023
Accepted 18 June 2023

Keywords:
Open-source framework
Cardiac magnetic resonance imaging
Computer-assisted methods
Heart diagnostic imaging
Image processing
Real-time imaging

ABSTRACT

In medicine, especially in radiology, artificial intelligence has sparked a growing interest in automated systems, image analysis, and acquisition standardization. In the wake of this standardization, the research field of "radiomics" has gained importance. Using computer-aided analysis, image data and contours can be evaluated to determine numerical values for shape, size, and gray-scale texture, which can then be examined in a clinical context. Especially in cardiovascular imaging, data acquisition and analysis in different cardiac and respiratory phases are of great interest. However, most research studies use parameters that have been laboriously calculated by hand. "ShortCardiac" is a Python-based framework with a user-friendly GUI for the quantitative determination of cardiac MR parameters. This allows researchers to utilize quantitative MR research for their studies without programming knowledge, with just a few clicks. All calculated parameters can be displayed graphically. "shortCardiac" allows the visualization of segmentation contours, the angle-dependent length measurement, the center of gravity and much more, in addition, the background can be hidden, and the images can be cropped automatically. In addition, "shortCardiac" can also be called via python and due to the object-oriented design, it is possible to integrate new segmentation frameworks with little effort in the future as well as to determine additional parameters. However, "ShortCardiac" comes with certain limitations. It only assesses cardiac short-axis data and functions merely as a post-processing framework for determining surrogate parameters based on segmentation and image information. Manual segmentations or usage of fully automated segmentations, such as Circle cvi42, require additional software tools. Regardless of these restrictions, "ShortCardiac" provides an efficient, user-friendly tool, enabling researchers to capitalize on the expanding domain of radiomics.

Code metadata

Current code version	*V1.0.1*
Permanent link to code/repository used for this code version	https://github.com/ElsevierSoftwareX/SOFTX-D-22-00407
Permanent link to reproducible capsule	https://github.com/MPR-UKD/shortCardiac/releases/tag/v1.0.1
Legal code license	*GNU General Public License (GPL)*
Code versioning system used	*GitHub*
Software code languages, tools and services used	*Python*
Compilation requirements, operating environments and dependencies	*Windows, Linux*
If available, link to developer documentation/manual	https://github.com/MPR-UKD/shortCardiac#readme
Support email for questions	MPR-UKD@med.uni-duesseldorf.de

1. Motivation and significance

In recent years, technological advances have led to the development of a variety of new biosensitive imaging techniques and post-processing algorithms [1–5], as well as new fast imaging techniques that allow real-time assessment of physiological processes [5–11]. These new techniques enable the acquisition of large datasets. As a result, there is a great interest in fully- or semi-automated evaluation pipelines [5,12,13], the research area "radiomics" [14–16], and Big Data analyses that

* Corresponding author.
E-mail address: ludger.radke@med.uni-duesseldorf.de (Karl Ludger Radke).

https://doi.org/10.1016/j.softx.2023.101453

provide radiologists with a comprehensive basis for evaluation [5,12,13,17,18].

The advantages of standardized evaluation pipelines and analysis algorithms are well known [15,19,20], and have been used and improved for years in quantitative MR studies, including Chemical Exchange Saturation Transfer (CEST) [21,22], Quantitative Susceptibility Mapping (QSM) [23], Diffusion tensor imaging (DTI) [24,25], and diffusion-weighted imaging (DWI) [26]. However, medical diagnostics, as well as numerous studies in which pathologies are analyzed exclusively without biosensitive imaging, are still based solely on visual analysis. This includes cardiac imaging. As a result, commercial software solutions such as Circle Cvi42 (Circle Cardiovascular Imaging Inc. Calgary, Canada) have been developed in recent years to improve visual representation of the heart. However, clinical research has also made progress in developing automatic methods for segmenting cardiac structures [27–29]. For example, Shaaf et al. proposed a fully convolutional neural network for automatic segmentation of the left ventricle from short-axis MRI images, which showed better segmentation performance compared to the standard U-mesh model [29]. However, segmentations alone are not of clinical utility, not until clinical surrogate parameters are determined based on them.

Therefore, this work aimed to develop an open-source framework for fast and standardized evaluation of cardiac short-axis magnetic resonance imaging (MRI) based on various surrogate parameters from previous studies, as well as the implementation of additional image contrast parameters, which enables a fully comprehensive quantification of MR data. The focus of the application is mainly on medical researchers without programming skills to allow entry into quantitative cardiac MRI using a few clicks, as well as a modular python pipeline for advanced users. We demonstrate the application of our tool to standard clinical MRI with an electrocardiogram (ECG) triggering and non-triggered real-time MRI of the beating heart, which allows comprehensive analysis of cardiac function under physiological conditions and is of research interest. In addition, we validate "shortCardiac" against manual references from an experienced radiologist.

2. Software description

The "shortCardiac" framework enables the semi-automatic determination of surrogate parameters for quantitative assessment of cardiac functionality based on short-axis MRI and is intended for scientific research only, especially it is not a medical product. It is distributed as a Jupyter notebook, Python source code (v3.7, Python Software Foundation, Wilmington, DE, USA), and user-friendly, stand-alone executable (.exe) graphical user interface (GUI) under the GNU General Public License (GPU GPL) license (GitHub: https://github.com/MPR-UKD/shortCardiac) and can be freely used and modified (Fig. 1 and Supplementary Figure S1).

The GUI allows a workflow adapted to the clinical work environment through easy navigation and graphical configuration of the evaluation pipeline (Fig. 1) and was developed in consultation with radiologists and cardiologists to facilitate operation. In addition, all calculations can be graphically visualized and saved between steps (Fig. 2).

For the determination, quantification, and evaluation of cardiac function, "shortCardiac" allows the automatic calculation of reference points, vectors, areas, and angle-dependent lengths, as well as the analysis of the eccentricity index (EI) based on previous cardiac studies [7,30–34]. In addition, "shortCardiac" allows the determination of five image feature classes: (1) first-order statistics, (2) non-angle-dependent shape descriptors, and (3) the Gray Level Co-occurrence Matrix (GLCM) texture feature, (4) Gray Level Run Length Matrix (GLRM), and (5) Gray Level Size Zone Matrix (GLSZM), which have led to the extraction of clinically relevant features in numerous previous studies [35–38]. The outlines can be segmented manually (e.g., with the ITK-Snap segmentation system [28]) or automatically with a framework (e.g., with the Deep Learning-based commercial software cvi42; Circle Cardiovascular Imaging Inc. Calgary, Canada).

2.1. Software architecture

As described above, "shortCardiac" is primarily designed for GUI operation. Nevertheless, "shortCardiac" follows a simple object-based architecture. There are four phases in the backend, whereby the actual calculation takes place in the fourth phase, and the other phases are used for preprocessing. The evaluation steps can be modified and extended via GUI and Source code. For this, no advanced programming knowledge is required; users only need to change the values using clicks within the GUI or modify the configuration file. For users with basic Python knowledge, our modular evaluation design allows for the straightforward addition of custom functions that return values and value names to be included in the saved CSV files (for more information, please see the GitHub Repository).

In the first phase, the coordinates and the corresponding DICOM images (cardiac MR images, X-ray images or computed tomography images in short-axis view) are read in, merged, and stored as a dictionary in Python pickle file format. In the subsequent second fully automated pre-processing step, the segmentations, which can be derived from any software that saves segmentations as NIFTI, such as ITK-SNAP; are checked, and consistent segmentation contours are ensured. This is done by determining polygon segmentations at a user-variable increased resolution as well as smoothing the contours, allowing for more accurate angle-based evaluation. In the third preprocessing step, the anatomical landmarks of the cranial and caudal transition of the interventricular septum into the RV are determined based on the endocardial contours of the right (RV) and left ventricle (LV) (Fig. 2a). The cardiac axis is vertically aligned (Fig. 2b and c) to allow calculation independent of the acquisition angle and thus standardized [7]. The fourth and final step (Fig. 2d–f) is divided into multiple independent functions to determine additional surrogate parameters.

In addition, "shortCardiac" has a debug mode in which individual intermediate steps can be visualized graphically. Furthermore, the functionality can be checked by unit tests. With the current default settings, 351 parameters are calculated per image. A detailed description of the individual post-processing methods can be found in the Jupyter notebook and source code.

2.2. Software functionalities

"shortCardiac" can be used for the evaluation of real-time MR recordings as well as for the evaluation of conventional MR recordings. "shortCardiac" supports two main functionalities: a user-friendly GUI, which can be executed either in a local Python environment or simply as *.exe, and the source-code-based evaluation. Here the use of the source code does not require advanced knowledge. As demonstrated in Figure S1, users can easily call "shortCardiac" using a simple script; they only need to define the DICOM folder and the coordinate file or NIFTI mask file. The evaluation as well as the reading, is executed fully automatically by the generation of class objects. The user only has to navigate independently through the file directory of his research project to evaluate larger amounts of data as well as to merge the patients \volunteers and the associated segmentations. Finally, all calculations are saved as a CSV file and can thus be easily analyzed subsequently.

Fig. 1. "ShortCardiac" framework with default settings. (Blue Box, 1) Main widget: In the pop-down widget at the top left, you can select how the coordinates have been segmented and which function is to be used to transfer the coordinates to a standardized file format. The "Load coordinates" and "Load DICOM-folder" buttons can then be used to read the coordinates and the DICOM images. The actual calculation is performed via the "Execute" button, and finally, the results are saved in a CSV file. (Red Box, 2) Widget for changing the configuration settings. (2.1) The parallelization can be adapted to the respective hardware and personnel requirements via the number of workers. The coordinates are scaled up with the rescaling factor for more accurate angle measurements. Furthermore, it can be activated that the heart angle should be corrected and whether the coordinates should be smoothed during rescaling. (2.2) Possibility to modify the angle-dependent measurements to the specific problem. (2.3) Determination of which texture analyses are to be performed. (2.4) Possibility to save the calculations as images to adapt them to individual personal requirements. (For interpretation of the references to color in this figure legend, the reader is referred to the web version of this article.)

3. Illustrative examples

To illustrate the use of "shortCardiac", a descriptive single-case observational study was designed with a healthy, 27-year-old male volunteer. The precipitant gave written informed consent and had no abnormalities of cardiac function after medical examination by D.K. (pediatric radiologist with 16 years of experience in cardiovascular MRI) and F.P. (clinical cardiologist with 20 years of experience). Approval from the local review board (Ethics Committee of the Medical Faculty of Heinrich Heine University, Düsseldorf, Germany 6176R) was obtained before the study. In addition, parts of the recorded data with anonymization of all nonrequired DICOM tags are deposited as a sample dataset in the GitHub repository.

3.1. Data acquisition

For the cardiac example MR measurements, the volunteer was positioned centrally in the MR scanner (1.5 T MAGNETOM Avanto fit, Siemens Healthineers, Erlangen, Germany) in the supine position, analogous to previous studies [6,7]. The MR protocol included a conventional retrospective ECG-gated cross-sectional MR measurement with a slice thickness of 8 mm, repetition time (TR) \echo time (TE) = 56.98/1.1 ms, and a flip angle of 73° with 14 slices along the short axis of the heart, as described in previous studies [6,7]. We also used a real-time gradient echo MRI sequence with pronounced radial undersampling and balanced steady-state free precession (bSSFP) contrast [6,11]. Acquisitions at the same slice positions as the conventional sequence provided a temporal resolution of 33.3 ms and a flip angle of 60° based on only 9 radial spokes.

3.2. Evaluation

For our data, we used the automatic segmentation tool of cvi42 (version 5.10.1. (1241); Circle Cardiovascular Imaging Inc. Calgary, Canada). While the automatic segmentation performed well in the middle slices, inaccuracies were observed towards the apex of the heart. To ensure accurate evaluation in all slices,

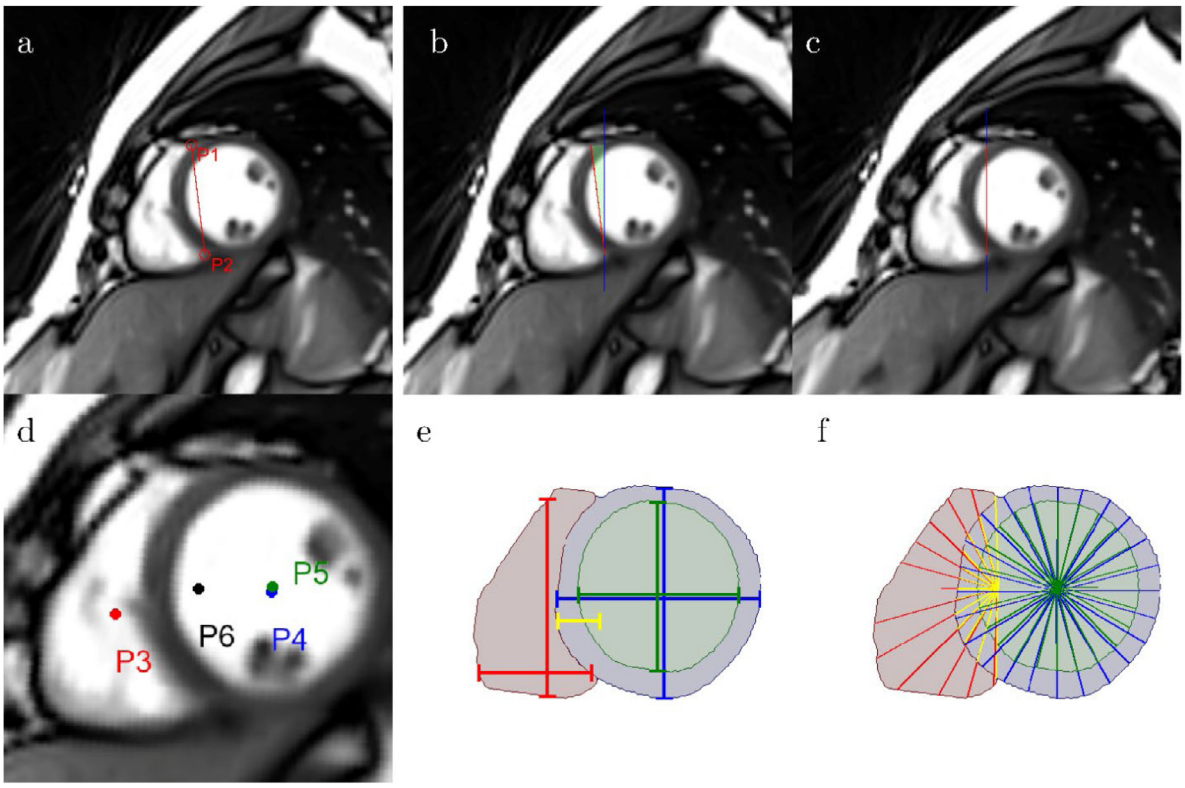

Fig. 2. Overview of specific surrogate parameters and standardized correction of cardiac alignment for a mid-ventricular slice of the real-time MRI. (a) Cranial (P1) and caudal (P2) reference points for cardiac alignment. (b) MR image before standardized cardiac alignment overlaid with the cardiac angle (green angle) of the septal axis (red) to the *y*-axis (blue) and after standardized correction of cardiac alignment (c). (d) Center of gravity of the endocardial contour of the right (P3, red) and left (P4, blue) ventricle, the epicardial contour of the left ventricle (P5, green), and the center point of the septal axis (P6, black). (e) Plotted straight lines for eccentricity index determination (red, blue, green). (f) Angle-dependent measurement of the cardiac contours. . (For interpretation of the references to color in this figure legend, the reader is referred to the web version of this article.)

all segmentations were subsequently checked (D.K.) and manually corrected using the freehand contouring tool. The GitHub repository also contains segmentations such as Nifti, such as those generated in the open-source ITK-Snap framework with the freehand polygon tool. Following the segmentation, the data were loaded into our tool and evaluated fully automatically. We used the GUI as well as the default settings for all calculations. Here, we had both the straight lines necessary for calculating the EI and the angle-dependent measurements saved as images (Figs. 3 and 4). As demonstrated in the figures, "shortCardiac" not only streamlines the calculation process but also offers an accessible way to visually verify the results. As depicted in Fig. 4, the background can be displayed with transparency, and 3D images can be generated as well.

For our healthy volunteer, in a midventricular slice of the RV and LV endocardium, we observed a periodic dependence of angle-dependent parameters, as expected. For the RV, we observed that different angular segments changed differently (Fig. 5a), and for the LV, the opposite lengths changed simultaneously (Fig. 5b). Compared with EI determination, angle-dependent evaluation allows more specific measurement of segments, which enables accurate mapping of elliptical shape (end-diastole) to a circular shape (end-systole) during cardiac phases of the LV. Similarly, we observed periodic changes in the other numerous radiomic features determined based on both contour and gray-scale image information, allowing quantitative analysis of cardiac phases (Fig. 5c).

3.3. Validation and accuracy of "shortCardiac"

One of the most important criteria for tool applicability, besides the ease of use shown in the previous one, is the accuracy compared to the current gold standard, i.e., time-consuming manual reference measurements. Using our real-time MRI data, we, therefore, performed statistical analyses to check the agreement between "shortCardiac" and an experienced radiologist. As described above, more than 1400 images were acquired using real-time analysis; because manual analysis of all images would be too time-consuming, 30 MR images were randomly selected and manually measured using the image analysis toolbox of the in-house image archiving and communication system (Sectra Workstation101, IDS7, Linköping, Sweden).

All subsequent statistical analyses were performed in R (v4.1.3, R Foundation for Statistical Computing) (K.L.R.). Both Bland–Altman plots and the intraclass correlation coefficient (ICC(2,1)) with a 95% confidence interval were used to assess the reliability of the automated analysis compared with the parameters [39]: (1) heart angle or septal alignment, (2) septal length corresponding to the length between reference points, and (3) left ventricular (LV-EI(endo)) and right ventricular eccentricity index (RV-EI(endo)) of the endocardium as well as left ventricular epicardium (LV-EI(epi)) as defined in previous studies.

The ICC was classified as poor (ICC $<$ 0.5), moderate (0.5 $\leq$ ICC $<$ 0.75), good (0.75 $\leq$ ICC $<$ 0.9), and excellent (ICC $\geq$ 0.9), according to Koo et al. [40]. Due to the experimental design of this study and the small sample size, the significance level of $p \leq 0.05$ was corrected to an adjusted significance level of $p \leq$

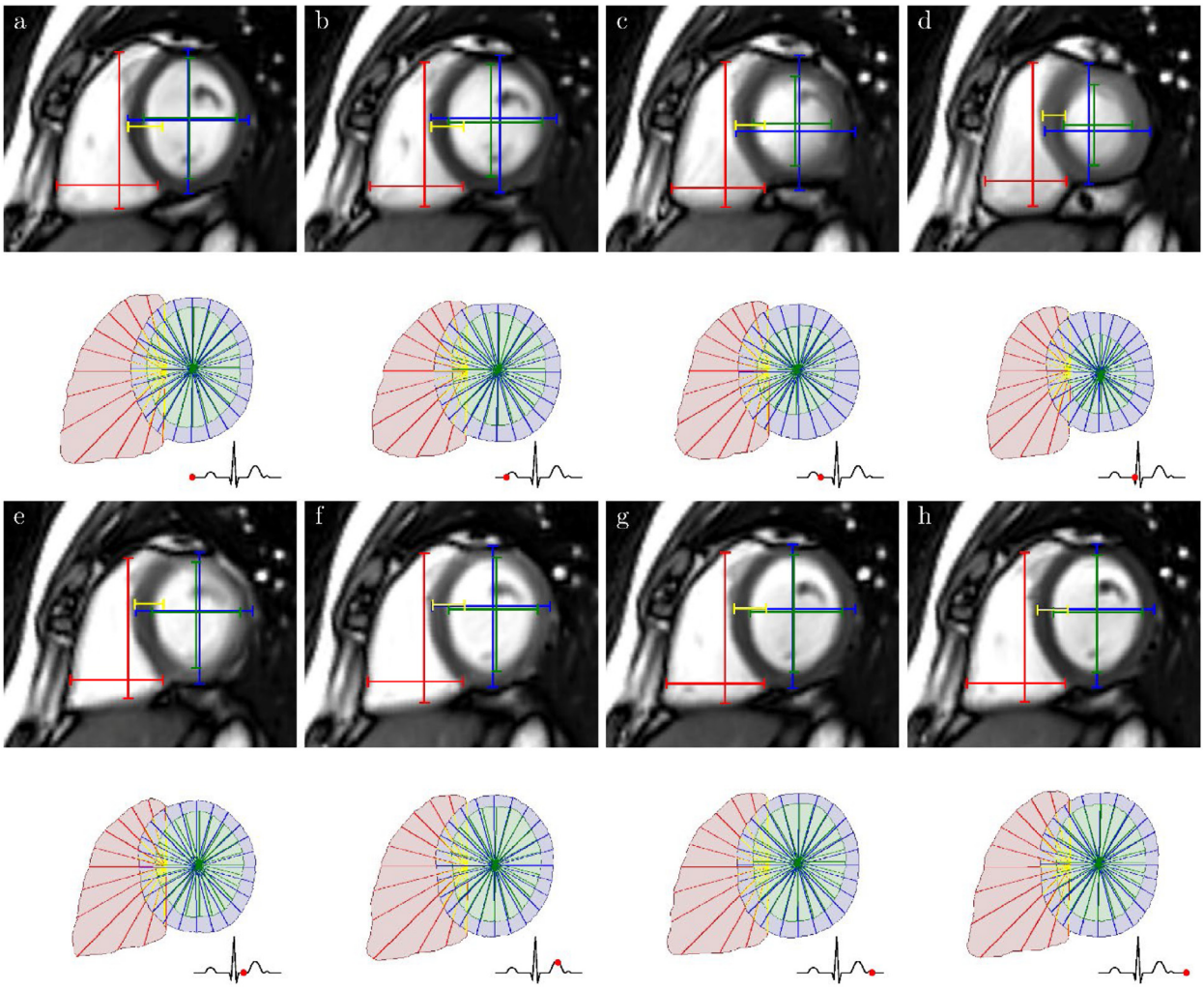

Fig. 3. Graphical visualization of 2D vector measurement using "shortCardiac". Shown are exemplary eight real-time MR images (a–h) presenting a complete cardiac cycle. The upper image shows the superimposed straight line of the RV-EI(endo) (red), the LV-EI(endo) (blue), the LV-EI(epi) (green), and the largest distance of the dorsal contour of the RV to the septum axis (yellow). The lower image shows in color the different segmented ROIs endocardium of the RV (red) and LV (green) as well as the epicardium of the LV (blue) and the angle-dependent length measurements (step size 15°). In addition, the red dot in the lower ECG signal shows the current time point in the cardiac cycle (ECG signals and time points are not to be scaled and are only for visualization purposes). In the supplementary Video S1, the same cardiac slice is shown as a video. (For interpretation of the references to color in this figure legend, the reader is referred to the web version of this article.)

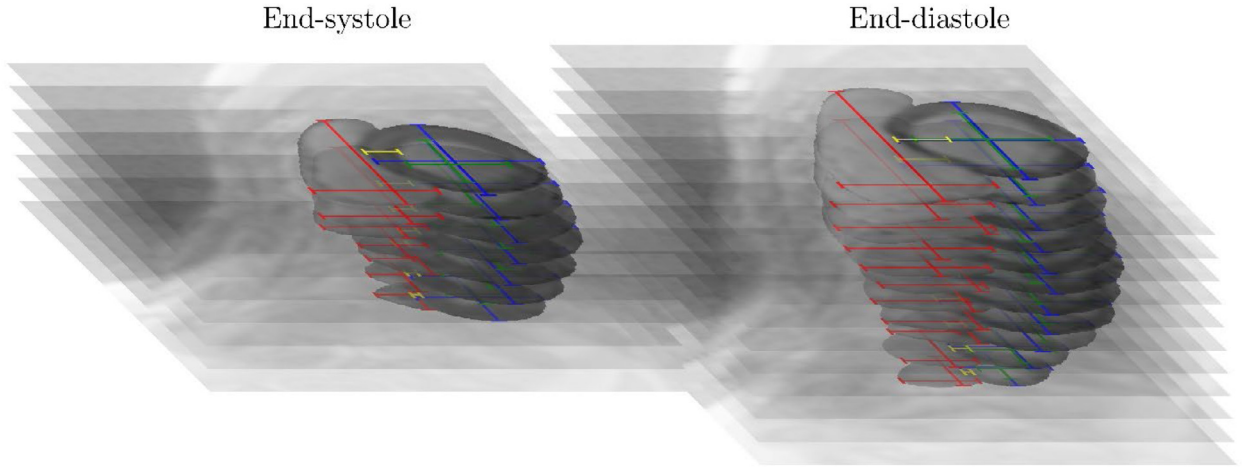

Fig. 4. 3D overlay of EI parameters determined with "shortCardiac" for the conventional 2D ECG-based MR measurements at end-diastole and end-systole. The areas outside the heart were presented transparently.

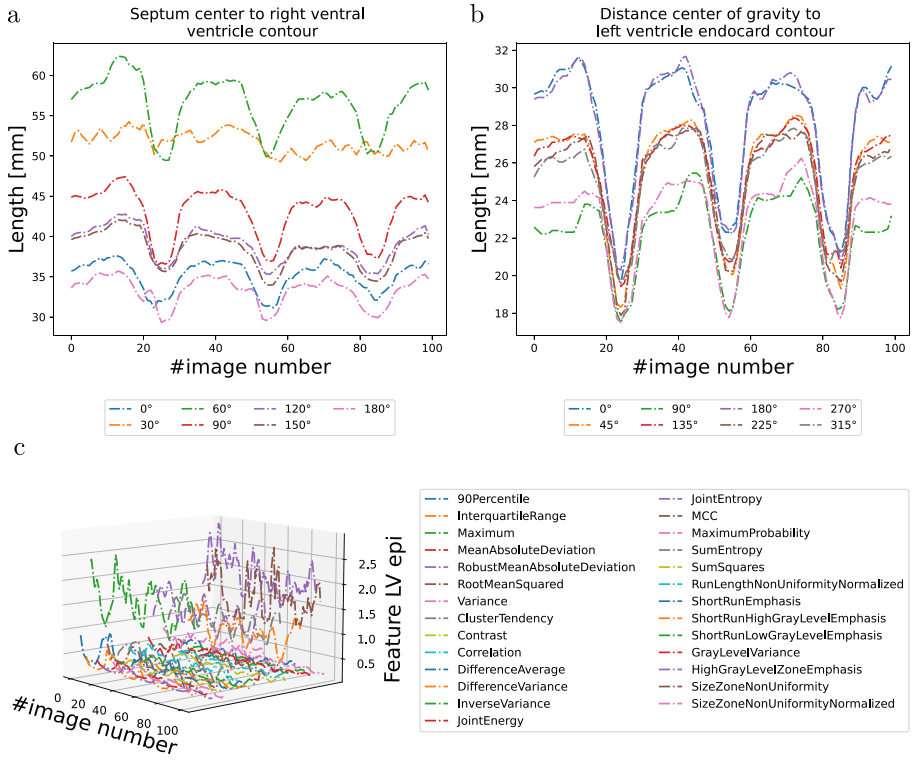

Fig. 5. Plot of some angle-dependent length parameters of the endocardial contours of the right (a) and left (b) ventricles and a selection of radiometric features as a function of time (cardiac phases), determined with "shortCardiac" and the first 100 real-time MR images. (a) For the right ventricle, different relative changes were observed as a function of the angular segments examined, indicating a change in ventricular shape during different cardiac phases. (b) For the left ventricle, it was found that at the end of systole, all angular segments are approximately the same distance from the center of gravity. Thus, the ventricle is circular. In contrast, at the end of diastole, there are significant differences in length between the angular segments, suggesting an elliptical shape. (c) In radiometric features, we observed analogous periodic changes that can be further investigated in later studies, possibly leading to different changes depending on disease or stage.

0.0125 using the conservative Bonferroni alpha adjustment [41]. This "low" significance level prevented inflation of the alpha error while maintaining statistical power.

For the automatic parameters, we observed excellent agreement with respect to the ICC(2,1) coefficient: the septal angle (ICC = 0.98; 95% CI = 0.97–0.99; $p < 0.0001$), septal length (ICC = 0.98; 95% CI = 0.96–0.99; $p < 0.0001$), RV-EI(endo) (ICC = 0.94; 95% CI = 0.87–0.97; $p < 0.0001$), LV-EI(endo) (ICC = 0.93; 95% CI = 0.86–0.97; $p < 0.0001$), and LV-EI(epi) (ICC = 0.91; 95% CI = 0.82–0.96; $p < 0.0001$). Bland–Altmann graphical analysis also shows near perfect agreement between "shortCardiac" and manual reference measurements (Fig. 6).

However, it should be emphasized that the evaluation by the radiologist took about 1 h, while "shortCardiac" required only 12 s for a complete evaluation.

Although very good accuracy was demonstrated in our validation dataset when evaluated with "shortCardiac", it is crucial to consider the impact of the DICOM data resolution on the accuracy of the calculated geometric parameters in "shortCardiac". Our software incorporates a scaling factor to enhance and stabilize angular measurements. However, it is worth noting that scaling results in contour smoothing, so images with too low resolution may yield deviating results in accuracy. "ShortCardiac" thus enables the user to save all calculated parameters graphically to visually verify the accuracy of the results. Moreover, the resolution of the DICOM data may also affect the precision of automatic segmentation methods in ITK-SNAP and other open-source as well as commercial programs. Consequently, segmentation contours should always be visually inspected by a user before evaluation, and if necessary, the contours should be manually corrected within the respective evaluation tools.

4. Impact

"ShortCardiac" enables fast and standardized evaluation of both real-time physiological MR measurements and ECG-triggered MR measurements. Using the Bland–Altmann plot and ICC, we validated the performance and accuracy of the presented framework compared to manual evaluation by an experienced radiologist. We can significantly reduce the evaluation time by parallelizing the image processing steps. While an experienced radiologist needs about one hour to acquire five clinically relevant features from a series of 30 images, "shortCardiac" needs only 12 s for the same images with the same accuracy. In addition, "shortCardiac" determines 351 parameters. The accelerated and computer-aided evaluation supports the analysis of large datasets, the acquisition of quantitative MR values as well as the reproducibility between research groups.

Analogous to the angle-dependent length measurements, which showed periodicity to cardiac phases in our study and in previous studies [7,30–34], we observed that periodic changes also occurred in parameters determined based on grayscale information. This allows a quantitative description of the image information and may lead to a better understanding and higher detection accuracy of pathologies in subsequent studies. In this regard, previous studies have successfully demonstrated that the determining features can provide additional clinically relevant information [35–38,42,43]. Among others, the study by Pinamonti et al. demonstrated the application of quantitative radiomics feature analysis of echocardiography data for the diagnosis of myocardial amyloidosis [44]. However, the radiomics approach also showed promise in feature analysis of cardio-computed tomography data [45,46]. In initial proof-of-concept studies, Baessler

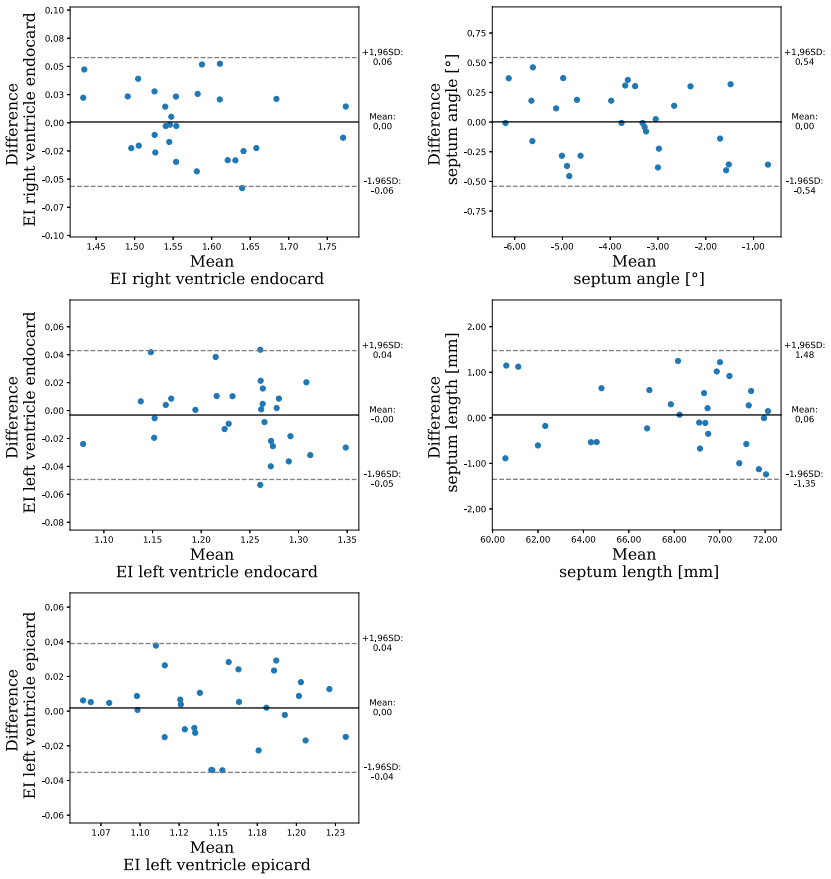

Fig. 6. Bland–Altman diagrams to evaluate the reliability between "shortCardiac" and the manual reference measurements of an experienced radiologist. Shown are the values of 30 randomly selected images from real-time MRI. The *y*-axes indicate the differences between "shortCardiac" and the reference measurement, while the *x*-axes indicate the mean value of the measures. The black lines indicate the mean values of the differences, and the gray dashed lines indicate the 95% confidence intervals.

et al. and other studies have shown that radiomic feature analysis of cardio MR data is able to accurately discriminate between myocardial disease and healthy hearts [45–47]. Compared with sophisticated biosensitive MR methods, radiomics allows easy application to routinely acquired data [42]. Further, this extraction of quantitative information enables a wide range of machine learning analyses, such as cluster analysis and regression algorithms.

In addition, evaluation using "shortCardiac" enables the full potential of real-time MRI, i.e., the temporal resolution of physiological processes [5–7]. Compared to conventional MRI, real-time imaging acquires too many images that can no longer be analyzed manually. Therefore, there is a great interest in automatic analysis tools such as "shortCardiac". In an earlier study, this made it possible, among other things, to perform a fully automatic and angle-dependent evaluation of wrists [5]. "shortCardiac" can be operated not only via GUI but also like an API interface, which supports the integration of "shortCardiac" into larger pipelines, in which, for example, the data is not segmented using a conventional software solution such as Circle, but by a deep-learning network optimized for its own application.

In addition, "shortCardiac" could be particularly useful in the analysis of large CMR datasets, as in the study of Raisi-Estabragh et al. in which the UK Biobank's cardiovascular magnetic resonance imaging data was explored by standardizing the analysis in an efficient way to gain valuable insights for the further development of cardiovascular research [18]. Furthermore, the application of "shortCardiac" can be extended to various clinical scenarios, as demonstrated by the study of Chen et al. highlighting the prognostic significance of left atrial and biventricular strain analysis in suspected myocarditis using cardiac magnetic resonance imaging in short axis view. Here, "shortCardiac" would provide more accurate analysis through fine angle-dependent measurement [43].

5. Conclusions

The open-source framework "ShortCardiac" offers a significant contribution to the field of clinical research by enabling fast, standardized evaluation of both real-time physiological MR measurements and ECG-triggered MR measurements. Our study has demonstrated the impressive performance and accuracy of this framework when compared to manual evaluation by an experienced radiologist, making it an invaluable tool for analyzing large datasets and ensuring reproducibility between research groups.

"ShortCardiac" not only reduces evaluation time through parallelized image processing steps but also provides an extensive range of 351 parameters, allowing for a more comprehensive understanding of pathologies in subsequent studies. The framework's potential for quantitative description of image information opens up opportunities for machine learning analyses, such as cluster analysis and regression algorithms.

Furthermore, "ShortCardiac" allows researchers to harness the full potential of real-time MRI and its temporal resolution of physiological processes. As conventional MRI is limited by the vast number of images that cannot be analyzed manually, the demand for automatic analysis tools like "ShortCardiac" is growing. The framework's versatility extends to its operation, supporting both GUI and API interfaces, thus facilitating its integration into larger pipelines.

In conclusion, the open-source framework "ShortCardiac", distributed under the GNU GPL license, provides an ideal working environment for clinical research. It allows for the extraction of surrogate parameters that can be used in subsequent studies to examine their changes and relevance to clinical questions. This powerful tool is freely available for use and modification, further promoting its widespread adoption in the field of quantitative cardiac MRI research.

Ethics approval and consent to participate

The study was conducted according to the guidelines of the Declaration of Helsinki and approved by the Institutional Review Committee of the Medical Faculty, University of Düsseldorf, Germany (protocol code study 6176R).

Consent for publication

Written informed consent was obtained from the healthy volunteer to publish this paper.

CRediT authorship contribution statement

Karl Ludger Radke: Conceptualization, Methodology, Software, Validation, Formal analysis, Investigation, Data curation, Writing – original draft, Visualization. **Janina Hußmann:** Conceptualization, Methodology, Writing – review & editing. **Lena Röwer:** Methodology, Validation, Writing – review & editing. **Dirk Voit:** Writing – review & editing. **Jens Frahm:** Writing – review & editing. **Gerald Antoch:** Writing – review & editing. **Dirk Klee:** Validation, Writing – review & editing. **Frank Pillekamp:** Conceptualization, Methodology, Formal analysis, Writing – Original Draft. **Hans-Jörg Wittsack:** Conceptualization, Methodology, Writing – original draft, Visualization, Supervision, Project administration.

Declaration of competing interest

The authors declare that they have no known competing financial interests or personal relationships that could have appeared to influence the work reported in this paper.

Data availability

Data will be made available on request.

Acknowledgments

We would like to thank the "Elterninitiative Kinderkrebsklinik e. V". for funding this research.

Appendix A. Supplementary data

Supplementary material related to this article can be found online at https://doi.org/10.1016/j.softx.2023.101453.

References

[1] Ramesh AN, Kambhampati C, Monson JRT, Drew PJ. Artificial intelligence in medicine. Ann R Coll Surg Engl 2004;86:334–8.
[2] Nedadur R, Wang B, Yanagawa B. The cardiac surgeon's guide to artificial intelligence. Curr. Opin Cardiol 2021;36:637–43.
[3] Davenport T, Kalakota R. The potential for artificial intelligence in healthcare. Future Healthc J 2019;6:94–8.
[4] Basu K, Sinha R, Ong A, Basu T. Artificial intelligence: How is it changing medical sciences and its future? Indian J Dermatol 2020;65:365–70.
[5] Radke KL, Wollschläger LM, Nebelung S, Abrar DB, Schleich C, Boschheidgen M, et al. Deep learning-based post-processing of real-time MRI to assess and quantify dynamic wrist movement in health and disease. Diagnostics (Basel, Switzerland) 2021;11.
[6] Röwer LM, Radke KL, Hußmann J, Malik H, Uelwer T, Voit D, et al. Comparison of cardiac volumetry using real-time MRI during free-breathing with standard cine MRI during breath-hold in children. Pediatr Radiol 2022;52:1462–75.
[7] Röwer LM, Uelwer T, Hußmann J, Malik H, Eichinger M, Voit D, et al. Spirometry-based reconstruction of real-time cardiac MRI: Motion control and quantification of heart-lung interactions. Magn Reson Med 2021;86:2692–702.
[8] Frahm J, Schätz S, Untenberger M, Zhang S, Voit D, Merboldt KD, et al. On the temporal fidelity of nonlinear inverse reconstructions for real- time MRI – the motion challenge. TOMIJ 2014;8:1–7.
[9] Krohn S, Gersdorff N, Wassmann T, Merboldt K-D, Joseph AA, Buergers R, et al. Real-time MRI of the temporomandibular joint at 15 frames per second-a feasibility study. Eur J Radiol 2016;85:2225–30.
[10] Uecker M, Zhang S, Voit D, Karaus A, Merboldt K-D, Frahm J. Real-time MRI at a resolution of 20 ms. NMR Biomed 2010;23:986–94.
[11] Voit D, Zhang S, Unterberg-Buchwald C, Sohns JM, Lotz J, Frahm J. Real-time cardiovascular magnetic resonance at 1.5 t using balanced SSFP and 40 ms resolution. J. Cardiovasc Magn Reson : Official J Soc Cardiovasc Magn Reson 2013;15:79.
[12] Qu J-H, Qin X-R, Li C-D, Peng R-M, Xiao G-G, Cheng J, et al. Fully automated grading system for the evaluation of punctate epithelial erosions using deep neural networks. Br J Ophthalmol 2021.
[13] Zhang J, Gajjala S, Agrawal P, Tison GH, Hallock LA, Beussink-Nelson L, et al. Fully automated echocardiogram interpretation in clinical practice. Circulation 2018;138:1623–35.
[14] Cui Y, Yin F-F. Impact of image quality on radiomics applications. Phys Med Biol 2022;67.
[15] Lambin P, Leijenaar RTH, Deist TM, Peerlings J, Jong EEC de, van Timmeren J, et al. Radiomics: the bridge between medical imaging and personalized medicine. Nature Rev Clin Oncol 2017;14:749–62.
[16] Mayerhoefer ME, Materka A, Langs G, Häggström I, Szczypiński P, Gibbs P, et al. Introduction to radiomics. Journal of nuclear medicine : official publication. Soc Nucl Med 2020;61:488–95.
[17] Hemmo Lotem M, Tzezana R, Levtzion-Korach O. The impact of artificial intelligence and big data on healthcare. Harefuah 2021;160:24–9.
[18] Raisi-Estabragh Z, Harvey NC, Neubauer S, Petersen SE. Cardiovascular magnetic resonance imaging in the UK biobank: A major international health research resource. Eur Heart J Cardiovasc Imag 2021;22:251–8.
[19] Rizzo S, Botta F, Raimondi S, Origgi D, Fanciullo C, Morganti AG, et al. Radiomics: the facts and the challenges of image analysis. Eur Radiol Exp 2018;2:36.
[20] Wilms LM, Radke KL, Abrar DB, Latz D, Schock J, Frenken M, et al. Micro- and macroscale assessment of posterior cruciate ligament functionality based on advanced MRI techniques. Diagnostics (Basel, Switzerland) 2021;11.
[21] Radke KL, Wilms LM, Frenken M, Stabinska J, Knet M, Kamp B, et al. Lorentzian-corrected apparent exchange-dependent relaxation (LAREX) Ω-plot analysis-an adaptation for qCEST in a multi-pool system: Comprehensive in silico, in situ, and in vivo studies. Int J Mol Sci 2022;23.
[22] Radke KL, Abrar DB, Frenken M, Wilms LM, Kamp B, Boschheidgen M, et al. Chemical exchange saturation transfer for lactate-weighted imaging at 3 t MRI: Comprehensive in silico, in vitro, in situ, and in vivo evaluations. Tomography (Ann Arbor, Mich.) 2022;8:1277–92.
[23] Bechler E, Stabinska J, Wittsack H-J. Analysis of different phase unwrapping methods to optimize quantitative susceptibility mapping in the abdomen. Magn Reson Med 2019;82:2077–89.
[24] Evertz R, Hub S, Backhaus SJ, Lange T, Toischer K, Kowallick JT, et al. Head-to-head comparison of different software solutions for AVC quantification using contrast-enhanced MDCT. J Clin Med 2021;10.
[25] Gholizadeh N, Greer PB, Simpson J, Denham J, Lau P, Dowling J, et al. Characterization of prostate cancer using diffusion tensor imaging: A new perspective. Eur J Radiol 2019;110:112–20.
[26] Hectors SJ, Semaan S, Song C, Lewis S, Haines GK, Tewari A, et al. Advanced diffusion-weighted imaging modeling for prostate cancer characterization: Correlation with quantitative histopathologic tumor tissue composition-A hypothesis-generating study. Radiology 2018;286:918–28.
[27] Dangi S, Yaniv Z, Linte CA. Left ventricle segmentation and quantification from cardiac cine MR images via multi-task learning. In: Pop M, Sermesant M, Zhao J, Li S, McLeod K, Young A, et al., editors. Statistical atlases and computational models of the heart: Atrial segmentation and LV quantification challenges : 9th International workshop, STACOM 2018, held in conjunction with MICCAI 2018, Granada, Spain, September 16, 2018 : Revised selected papers, Vol. 11395. Cham: Springer; 2019, p. 21–31.

[28] Yushkevich PA, Piven J, Hazlett HC, Smith RG, Ho S, Gee JC, et al. User-guided 3D active contour segmentation of anatomical structures: significantly improved efficiency and reliability. NeuroImage 2006;31:1116–28.
[29] Shaaf ZF, Jamil MMA, Ambar R, Alattab AA, Yahya AA, Asiri Y. Automatic left ventricle segmentation from short-axis cardiac MRI images based on fully convolutional neural network. Diagnostics (Basel, Switzerland) 2022;12.
[30] Yamasaki Y, Nagao M, Kamitani T, Yamanouchi T, Kawanami S, Yamamura K, et al. Clinical impact of left ventricular eccentricity index using cardiac MRI in assessment of right ventricular hemodynamics and myocardial fibrosis in congenital heart disease. Eur Radiol 2016;26:3617–25.
[31] Oşvar FN, Raţiu AC, Voiţă-Mekereş F, Voiţă GF, Bonţea MG, Racoviţă M, et al. Cardiac axis evaluation as a screening method for detecting cardiac abnormalities in the first trimester of pregnancy. 2020;61:137–42.
[32] Grapsa J, Dawson D, Nihoyannopoulos P. Assessment of right ventricular structure and function in pulmonary hypertension. J Cardiovasc Ultrasound 2011;19:115–25.
[33] Wang L, Chen X, Wan K, Gong C, Li W, Xu Y, et al. Diagnostic and prognostic value of right ventricular eccentricity index in pulmonary artery hypertension. Pulm Circulation 2020;10:2045894019899778.
[34] Gimelli A, Liga R, Clemente A, Marras G, Kusch A, Marzullo P. Left ventricular eccentricity index measured with SPECT myocardial perfusion imaging: An additional parameter of adverse cardiac remodeling. J Nucl Cardiol : Official Publ Am Soc Nucl Cardiol 2020;27:71–9.
[35] Araujo Faria V de, Azimbagirad M, Viani Arruda G, Fernandes Pavoni J, Cezar Felipe J, Dos Santos EMCMF, et al. Prediction of radiation-related dental caries through PyRadiomics features and artificial neural network on panoramic radiography. J Digit Imaging 2021;34:1237–48.
[36] Zwanenburg A, Vallières M, Abdalah MA, Aerts HJWL, Andrearczyk V, Apte A, et al. The image biomarker standardization initiative: Standardized quantitative radiomics for high-throughput image-based phenotyping. Radiology 2020;295:328–38.
[37] Raisi-Estabragh Z, Jaggi A, Gkontra P, McCracken C, Aung N, Munroe PB, et al. Cardiac magnetic resonance radiomics reveal differential impact of sex, age, and vascular risk factors on cardiac structure and myocardial tissue. Front Cardiovasc Med 2021;8:763361.
[38] Ayx I, Tharmaseelan H, Hertel A, Nörenberg D, Overhoff D, Rotkopf LT, et al. Comparison study of myocardial radiomics feature properties on energy-integrating and photon-counting detector CT. Diagnostics (Basel, Switzerland) 2022;12.
[39] Shrout PE, Fleiss JL. Intraclass correlations: Uses in assessing rater reliability. Psychol Bull 1979;86:420–8.
[40] Koo TK, Li MY. A guideline of selecting and reporting intraclass correlation coefficients for reliability research. J Chiropr Med 2016;15:155–63.
[41] Armstrong RA. When to use the Bonferroni correction. Ophthalmic Physiol Opt : J Br Coll Ophthalmic Opticians (Optometrists) 2014;34:502–8.
[42] Raisi-Estabragh Z, Izquierdo C, Campello VM, Martin-Isla C, Jaggi A, Harvey NC, et al. Cardiac magnetic resonance radiomics: basic principles and clinical perspectives. Eur Heart J Cardiovasc Imag 2020;21:349–56.
[43] Chen Y, Zhao W, Zhang N, Liu J, Liu D, Sun Z, et al. Prognostic significance of cardiac magnetic resonance in left atrial and biventricular strain analysis during the follow-up of suspected myocarditis. J Clin Med 2023;12.
[44] Pinamonti B, Picano E, Ferdeghini EM, Lattanzi F, Slavich G, Landini L, et al. Quantitative texture analysis in two-dimensional echocardiography: Application to the diagnosis of myocardial amyloidosis. J Am Coll Cardiol 1989;14:666–71.
[45] Oikonomou EK, Williams MC, Kotanidis CP, Desai MY, Marwan M, Antonopoulos AS, et al. A novel machine learning-derived radiotranscriptomic signature of perivascular fat improves cardiac risk prediction using coronary CT angiography. Eur Heart J 2019;40:3529–43.
[46] Kolossváry M, Kellermayer M, Merkely B, Maurovich-Horvat P. Cardiac computed tomography radiomics: A comprehensive review on radiomic techniques. J Thorac Imaging 2018;33:26–34.
[47] Baeßler B, Mannil M, Maintz D, Alkadhi H, Manka R. Texture analysis and machine learning of non-contrast T1-weighted MR images in patients with hypertrophic cardiomyopathy-preliminary results. Eur J Radiol 2018;102:61–7.